Structure, Rotational Dynamics, and Superfluidity of Small OCS-Doped He Clusters

Saverio Moroni,[1] Antonio Sarsa,[2,*] Stefano Fantoni,[2] Kevin E. Schmidt,[2,†] and Stefano Baroni[2,3,‡]

[1]*SMC INFM–Istituto Nazionale per la Fisica della Materia and Dipartimento di Fisica, Università di Roma La Sapienza, Piazzale Aldo Moro 2, I-00185 Rome, Italy*

[2]*SISSA and INFM DEMOCRITOS National Simulation Center, Via Beirut 2-4, I-34014 Trieste, Italy*

[3]*Chemistry Department, Princeton University, Princeton, New Jersey 08544*

(Received 11 December 2002; published 10 April 2003)

The structural and dynamical properties of carbonyl sulfide (OCS) molecules solvated in helium clusters are studied using reptation quantum Monte Carlo, for cluster sizes $n = 3$–20 He atoms. Computer simulations allow us to establish a relation between the rotational spectrum of the solvated molecule and the structure of the He solvent, and of both with the onset of superfluidity. Our results agree with a recent spectroscopic study of this system and provide a more complex and detailed microscopic picture of this system than inferred from experiments.

DOI: 10.1103/PhysRevLett.90.143401 PACS numbers: 36.40.Mr, 61.46.+w, 67.40.Yv

Solvation of molecules in He nanodroplets provides a way to study their properties in an ultracold matrix and offers the opportunity to probe the physics of quantum fluids in confined geometries. Research in this field has been recently reviewed in Ref. [1], with emphasis on experiment and hydrodynamic modeling, and in Ref. [2], with emphasis on computer simulations.

Carbonyl sulfide (OCS) is one of the most widely studied dopants of He clusters (OCS@He_n) [2–5], both because of its strong optical activity in the infrared and microwave spectral regions, and also because the OCS@He_1 complex is spectroscopically well characterized [6,7], thus providing a solid benchmark for the atom-molecule interaction potential which is the key ingredient of any further theoretical investigation.

In the quest of fingerprints of superfluidity in the spectra of small- and intermediate-size He clusters, Tang *et al.* have recently determined the vibrational and rotational spectra of OCS@He_n at high resolution for $n =$ 2–8 [3]. The main results of that investigation are (i) the rotational constant of the solvated molecule roughly equals the nanodroplet (large-n) limit [8] at $n = 5$, but then undershoots this asymptotic value up to the maximum cluster size ($n = 8$) attained in that work; (ii) the centrifugal distortion constant has a minimum at $n = 5$, thus suggesting that the complex is more rigid at this size; (iii) the fundamental vibrational frequency of OCS is not a monotonic function of n, but it displays a maximum at $n = 5$, again indicating a stronger rigidity at this size. Findings (ii) and (iii) suggest—and our study of the rotational spectra confirms—that $n = 5$ is a magic size related to the structure of solvent atoms around the solvated molecule. Finding (i) implies the existence of a (yet to be determined) minimum in the rotational constant as a function of the cluster size. The occurrence of this minimum was interpreted as due to quantum exchanges which would decrease the effective inertia of the first solvation shell and would thus signal the onset of *superfluidity* in this finite system [3].

Quantum simulations are complementary to experiments for understanding the properties of matter at the atomic scale. In fact, while being limited by our incomplete knowledge of the interatomic interactions and by the size of the systems one can examine, simulations provide a wealth of detailed information which cannot be obtained in the laboratory. In this paper we show how quantum Monte Carlo simulations can be used to get an unparalleled insight into the exotic properties of small He clusters. Also, some of the dynamical properties thus predicted are so sensitive to the details of the atom-molecule interactions that they provide an accurate test of the available model potentials.

The structure and the rotational dynamics of OCS@He_n clusters are studied here in the small-to-intermediate size regime ($n = 3$–20), using *reptation quantum Monte Carlo* (RQMC) [9], a technique by which ground-state properties (such as the density distribution and various static and dynamic correlations) can be determined with high accuracy. In particular, the analysis of the dynamical dipole correlation function allows us to resolve several rotational components of the spectrum of this interacting quantum system. RQMC combines the best features of the path-integral (PIMC) and diffusion quantum Monte Carlo (DQMC) techniques, yet avoiding some of their drawbacks: RQMC is not affected by the systematic errors which plague the estimate of ground-state expectation values in DQMC (the so-called mixed-estimate and population-control biases) and gives easy access to time correlations, from which dynamical properties can be extracted [9]; at the same time, the RQMC technique is specially tailored to the zero-temperature (ground-state) regime, where PIMC becomes inefficient.

The He-He and the He-OCS interactions used here are derived from quantum-chemical calculations [10,11]. The OCS molecule is assumed to be rigid. The trial wave function is chosen to be of the Jastrow form: $\Phi_T = \exp[-\sum_{i=1}^{n} \mathcal{U}_1(r_i, \theta_i) - \sum_{i<j}^{n} \mathcal{U}_2(r_{ij})]$, where r_{ij} is the

distance between the ith and the jth helium atoms, $r_i = |\mathbf{r}_i|$ is the distance of the ith atom from the center of mass of the molecule, and θ_i is the angle between the molecular axis and $\mathbf{r}_i$. $\mathcal{U}_1$ is expanded as a sum of five products of radial functions times Legendre polynomials. All radial functions (including $\mathcal{U}_2$) are optimized independently for each cluster size with respect to a total of 27 variational parameters. The propagation time is set to 1 K^{-1}, with a time step of 10^{-3} K^{-1}. The effects of the length of the time step and of the projection time [9] have been tested by simulations performed by halving the former or doubling the latter, resulting in negligible changes compared to the statistical errors.

The absorption spectrum of a molecule solvated in a nonpolar environment is given by the Fourier transform of the autocorrelation function of its dipole, $\mathbf{d}$: $I(\omega) \propto 2\pi \sum_n |\langle\Psi_0|\mathbf{d}|\Psi_n\rangle|^2 \delta(E_n - E_0 - \omega) = \int e^{i\omega t}\langle\mathbf{d}(t)\cdot\mathbf{d}(0)\rangle dt$, where Ψ_0 and Ψ_n are ground- and excited-state wave functions of the system, E_0 and E_n the corresponding energies, and $\langle\cdot\rangle$ indicates ground-state expectation values. The dipole of a linear molecule—such as OCS—is oriented along its axis, so that the optical activity is essentially determined by the autocorrelation of the molecular orientation vector: $c(t) = \langle\mathbf{n}(t)\cdot\mathbf{n}(0)\rangle$. Within RQMC the analytical continuation to the imaginary time of $c(t)$, $\bar{c}(\tau) = c(-i\tau)$, can be conveniently calculated without any other approximations than those implicit in the use of a given parametrization of the interatomic potentials [9]. From now on, when referring to *time correlation functions*, we will mean quantum correlations in imaginary time, and we will drop the bar over $\bar{c}(\tau)$. Continuation to imaginary time transforms the oscillations of the real-time correlation function—which are responsible for the δ-like peaks in its Fourier transform—into a sum of decaying exponentials whose decay constants are the excitation energies, $E_n - E_0$, and whose spectral weights are proportional to the absorption oscillator strengths, $|\langle\Psi_0|\mathbf{d}|\Psi_n\rangle|^2$. Dipole selection rules imply that only states with $J = 1$ can be optically excited from the ground state. Information on excited states with different angular momenta, J, can be easily extracted from the multipole correlation functions, $c_J(\tau)$, defined as the time correlations of the Legendre polynomials: $c_J(\tau) = \langle P_J(\mathbf{n}(\tau)\cdot\mathbf{n}(0))\rangle \equiv (4\pi)/(2J+1) \times \langle\sum_{M=-J}^{J} Y^*_{JM}(\mathbf{n}(\tau))Y_{JM}(\mathbf{n}(0))\rangle$. For each value of J, the value of the lowest-lying excitation energy, ϵ_J^1, i.e., the smallest decay constant in $c_J(\tau)$, as well as the corresponding spectral weight, A_J^1, can be extracted from a fit to $c_J(\tau)$. We have verified that the values so obtained are rather insensitive to the details of the fitting procedure.

In Fig. 1 we display multipole correlations calculated up to $J = 5$ for OCS@He_5 and OCS@He_{10}. For a rigid top, time correlations are described by a single exponential for each value of J, $c_J(\tau) = e^{-\epsilon_J\tau}$, with $\epsilon_J = BJ(J+1)$. The rigid-top energy levels are displayed as dashed lines. Time correlations deviate from this behavior at short times, thus indicating that the nonrigidity of the cluster affects the spectra only at high frequencies, the deviation being larger for larger J. The dependence of ϵ on J is well predicted by the rigid-top model for $n = 5$, while it is less so for $n = 10$. In all cases, the excitation energies are well described by a formula containing an effective centrifugal distortion constant: $\epsilon_J = BJ(J+1) - DJ^2(J+1)^2$ [12].

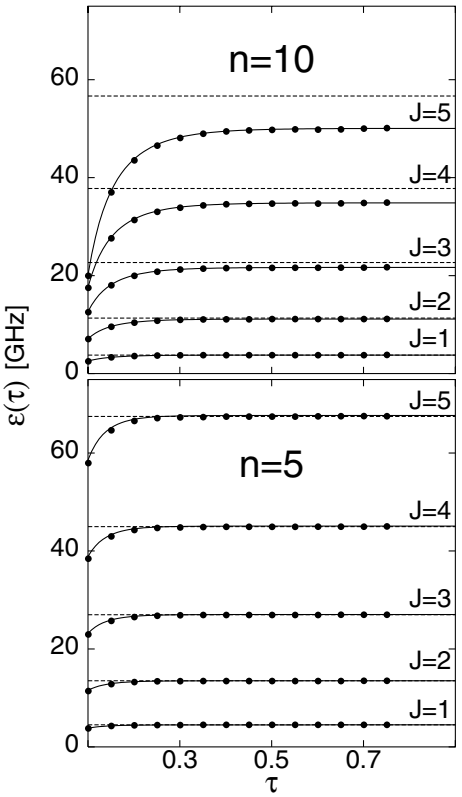

FIG. 1. Logarithm of the multipole correlation function, normalized by the spectral weight of the lowest-lying state: $\epsilon(\tau) = -\log(c_J(\tau)/A_J^1)/\tau$, for $n = 10$ (upper panel) and $n = 5$ (lower panel). Time units are K^{-1}.

In Fig. 2 we display the rotational constant, B, and centrifugal distortion constant, D, as functions of the cluster size. B displays a minimum at $n = 8$–9 [13], while D is minimum at $n = 5$, indicating a greatest rigidity of the OCS@He complex at this size. In order to discuss these findings and their relation with the structure of the cluster, with the onset of superfluidity, and with the quality of the interaction potential used for the simulation, we first define $\rho(\mathbf{r})$ as the He number-density distribution, and $\phi(\mathbf{r})$ as the ground-state expectation value of molecule-atom angular motion correlation: $\phi(\mathbf{r}) = -\langle\Psi_0|\mathbf{L}\cdot\mathbf{l}(\mathbf{r})|\Psi_0\rangle$. In this expression $\mathbf{L}$ indicates the angular momentum of the OCS molecule and $\mathbf{l}(\mathbf{r})$ is the angular-current operator of He atoms at point $\mathbf{r}$: $\mathbf{l}(\mathbf{r}) = -i\hbar\mathbf{r}\times\sum_l[(\partial/\partial\mathbf{r}_l)\delta(\mathbf{r}-\mathbf{r}_l) + \delta(\mathbf{r}-\mathbf{r}_l)(\partial/\partial\mathbf{r}_l)]$. The angular correlation function, $\phi(\mathbf{r})$, is non-negative and it is large whenever the angular motion of He atoms at point $\mathbf{r}$ is strongly correlated with the rotation of the

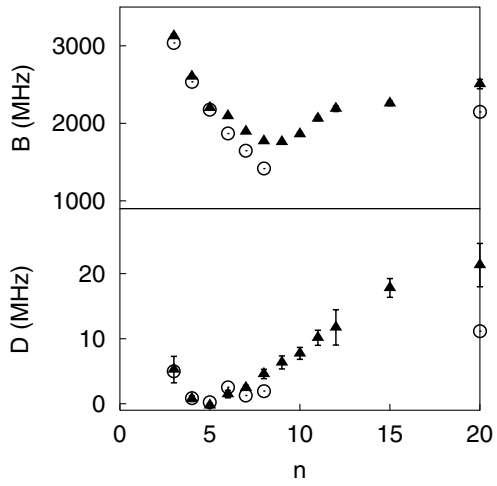

FIG. 2. Rotational constants (upper panel) and rotational distortion constant (lower panel, see text) of OCS@He_n, as functions of the cluster size, n. Triangles indicate the results of the present simulation (error bars are smaller than the triangles, when they are not visible), whereas circles are experimental data from Ref. [3].

solvated molecule, thus contributing to the molecular effective moment of inertia.

In Fig. 3 we display $\rho(\mathbf{r})$ and $\phi(\mathbf{r})$, as calculated for cluster sizes $n = 5$, 8, 10, and 15. The He density reaches its maximum where the He-OCS interaction potential is minimum, i.e., in a *doughnut* surrounding the molecule perpendicular to the OC bond. This doughnut can accommodate up to five He atoms which rotate rather rigidly with the OCS molecule, as demonstrated by the large value of the angular correlation function. Each atom within the doughnut gives the same contribution to the cluster moment of inertia, resulting in a constant slope of B vs n for $n \leq 5$. Secondary minima of the He-OCS potential exist near the two poles, the one nearest to the S atom being deeper. For $n > 5$ He atoms spill out of the main minimum and spread towards other regions of space, preferentially near the molecular poles.

An analysis of the He density plots for $n = 6$, 7, and 8 shows that—due to quantum tunneling to and from the doughnut—both polar regions start to be populated as soon as the doughnut occupation is completed (i.e., for $n > 5$). The number of He atoms near the S pole is 0.2, 0.3, and 0.7, for $n = 6$, 7, and 8, and 0.5, 0.8, and 1.1 near the O pole. The He density is larger near the O pole because both a smaller energy barrier and a smaller distance favor quantum tunneling.

Tunneling is the key for understanding the onset of superfluidity, as well as the sensitivity of rotational spectra to the details of the He-OCS interaction. For $n = 6$, 7, and 8, a sizable He density is found not only near the molecular poles, but also in the angular region between the doughnut and the O pole, where the energy barrier is small. Non-negligible angular correlations indicate that atoms in this region (and not only near the poles) contribute to the effective moment of inertia. For $n > 8$ He atoms start to fill the region between the doughnut and the S pole (see the $n = 10$ panel of Fig. 3). The closure of He rings in the sagittal planes makes atomic exchanges along these rings possible, thus triggering the same mechanism responsible for superfluidity in infinite systems [14]. The onset of superfluidity is responsible not only for negligible angular correlations in this region, but also for the decrease of these correlations in the doughnut where the largest contributions to the cluster inertia come from. This is demonstrated in the bottom-right panel of Fig. 3, which shows that the maximum of the angular correlation in the doughnut region starts decreasing for $n > 8$.

It is interesting to examine the dependence upon cluster size of the spectral weights, A_J^ν. The A_J^ν's are positive and they sum to 1: a value of A_J^1 close to 1 indicates that few rotational states are available to couple with the lowest-lying excitation of the molecule (in the case of a rigid top, there is only one state per angular momentum, and $A_J^1 = 1$). For $J = 1$ A_J^1 displays a maximum at $n = 4$–5—where the cluster is stiffest—and a minimum at $n = 8$; for $n = 20$ the value of A_1^1 roughly equals the

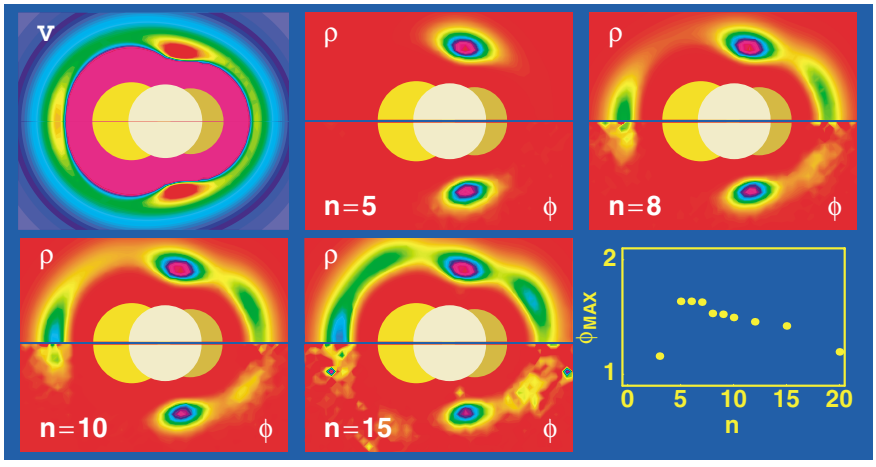

FIG. 3 (color). Upper left panel: He-OCS interaction potential. The atoms constituting the molecule are displayed as circles whose radius is the corresponding van der Waals radius (sulphur on the left). Panels with red background: upper half, He number density; lower half, angular motion correlation function (see text). Colors go from red to violet, as in a rainbow, as the value of the function increases. Lower right panel: maximum of the angular motion correlation function, as a function of the cluster size.

maximum attained at $n = 4$–5. We interpret the rise of A_1^1 for $n > 8$ as due to a decrease of the number of low-lying excited states of the solvent, in strict analogy to the mechanism responsible for superfluidity in the bulk [14]. For $J = 5$, A_J^1 decreases monotonically for $n > 5$, suggesting that, due to the larger excitation energy, many states of the solvent are available to couple with the molecular rotation in this case.

This quantum tunneling makes the rotational constants for $n > 5$ rather sensitive to the height and width of the barriers between different minima of the OCS-He interaction potential. On the other hand, the details of the potential off the main minimum in the doughnut hardly affect the spectra for $n \leq 5$ and, in particular, that of $OCS@He_1$ which is used as a benchmark for the quality of the potential [11]. Our simulations predict rotational constants which are in excellent agreement with experiment for $n \leq 5$, while for $n \geq 6$ the predicted values of B are too large and display too small a slope as a function of n. We believe that both these facts are due to the smallness of the barriers between the main and the secondary energy minima, which determines an excessive spillout of He atoms off the main minimum for $n = 6$ and an excessive propensity towards atomic exchanges for $n \geq 6$. We expect that larger energy barriers would result in a better agreement between theory and experiment for $6 \leq n \leq 8$ and, possibly, in a shift of the predicted minimum of the rotational constant towards larger sizes. As a qualitative test, we have done some simulations with a uniformly scaled potential ($V_{\text{He-OCS}} \rightarrow \alpha V_{\text{He-OCS}}$). Although not very realistic, this transformation copes with the possible drawbacks of the potential by raising the barriers while leaving the location of the minima unchanged. For $\alpha = 1.2$, we find that the values of B for $n \leq 5$ are left practically unchanged, while the agreement with experiment is much improved for $n = 6$, 7, and 8. The resulting minimum value of B stays located near $n = 8$–9. This seems to indicate that the location of the minimum is rather insensitive to the details of the He-OCS potential.

In conclusion, quantum simulations explain the relation existing among structure, dynamics, and superfluidity in small doped He clusters, and provide a sensitive test of the quality of atom-molecule potentials, in regions which hardly affect the spectra of the monatomic molecular complex.

We thank W. Jäger for sending us a preprint of Ref. [3] prior to publication and G. Scoles for bringing that work to our attention and for a careful reading of the first draft of the present paper. S. B. thanks K. Lehman and G. Scoles for many illuminating discussions held at the Chemistry Department of the Princeton University during two extended visits to R. Car. We thank F. A. Gianturco for his interest in our work and for providing us with a preprint of Ref. [5](b) prior to publication. This work was partially supported by the Italian MIUR (PRIN 2000 and 2001), by the U.S. ONR (Grant No. N00014-01-1-1061), and by the Spanish *Ministerio de Ciencia y Tecnologia* (Contract No. BMF2002-00200).

*Present address: Departamento de Fisica Moderna, Universidad de Granada, E-18071 Granada, Spain.
†Permanent address: Department of Physics and Astronomy, Arizona State University, Tempe, AZ 85287.
‡Permanent address: SISSA and DEMOCRITOS, Trieste, Italy.

[1] C. Callegari, K. K. Lehmann, R. Schmied, and G. Scoles, J. Chem. Phys. **115**, 10 090 (2001).
[2] Y. Kwon, P. Huang, M.V. Patel, D. Blume, and K. B. Whaley, J. Chem. Phys. **113**, 6469 (2000).
[3] J. Tang, Y. J. Xu, A. R.W. McKellar, and W. Jäger, Science **297**, 2030 (2002).
[4] F. Paesani, F. A. Gianturco, and K. B. Whaley, J. Chem. Phys. **115**, 10 225 (2001); Y. Kwon and K. B. Whaley, J. Chem. Phys. **115**, 10 146 (2001).
[5] (a) F. Paesani, F. A. Gianturco, and K. B. Whaley, Europhys. Lett. **56**, 658 (2001); (b) F. Paesani, A. Viel, F. A. Gianturco, and K. B. Whaley, Phys. Rev. Lett. **90**, 073401 (2003).
[6] K. Higgins and W. Klemperer, J. Chem. Phys. **110**, 1383 (1999).
[7] J. Tang and A. R.W. McKellar, J. Chem. Phys. **115**, 3053 (2001).
[8] S. Grebenev, J. P. Toennies, and A. F. Vilesov, Science **279**, 2083 (1998).
[9] S. Baroni and S. Moroni, Phys. Rev. Lett. **82**, 4745 (1999); in *Quantum Monte Carlo Methods in Physics and Chemistry*, edited by P. Nightingale and C. J. Umrigar, NATO ASI, Ser. C, Vol. 525 (Kluwer Academic Publishers, Boston, 1999), p. 313 (see also http://xxx.lanl.gov/abs/cond-mat/9808213).
[10] T. Korona, H. L. Williams, R. Bukowski, B. Jeziorski, and K. Szalewicz, J. Chem. Phys. **106**, 5109 (1997).
[11] J. M. M. Howson and J. M. Hutson, J. Chem. Phys. **115**, 5059 (2001).
[12] The evaluation of the distortion constant, D, is much facilitated by the large correlations existing among the time series from which the $c_J(\tau)$'s are extracted for different values of J (they all derive from a same underlying random walk). Because of this, the statistical error in the ratio of any two c_J's (whose logarithmic derivatives give excitation energies) is smaller than the error on individual c_J's.
[13] A study of B as a function of n has also been reported in Ref. [5(b)] using a different method and a different potential, and leading to somewhat different results (the main difference being that the minimum of B is found to occur at $n = 6$).
[14] R. P. Feynman, Phys. Rev. **91**, 1291 (1953); **91**, 1301 (1953).